Neon and Helium in the Surface of Stardust Cell C2028

R. L. Palma[1,2], R. O. Pepin[2], D. J. Schlutter[2], D. R. Frank[3], R. Bastien[3], and M. Rodriguez[3]

[1]Minnesota State University, Mankato MN, USA. [2]University of Minnesota, Minneapolis MN, USA. [3]NASA-JSC, Houston TX, USA.

Introduction

Previous He and Ne studies in Stardust aerogel samples detected a variety of non-terrestrial compositions [1-4]. However, except for materials keystoned from Track 41 in cell C2044 [1,2], none of these samples contained observable fragments of Wild 2 comet coma grains [3,4]. Here we report light noble gas data from analyses of surface samples of aerogel cell C2028. The surface of this cell is riddled with shallow tracks containing small terminal particles thought to be secondary in origin, ejected toward the cell when a parent grain collided with the spacecraft structure and fragmented.

Results and Discussion

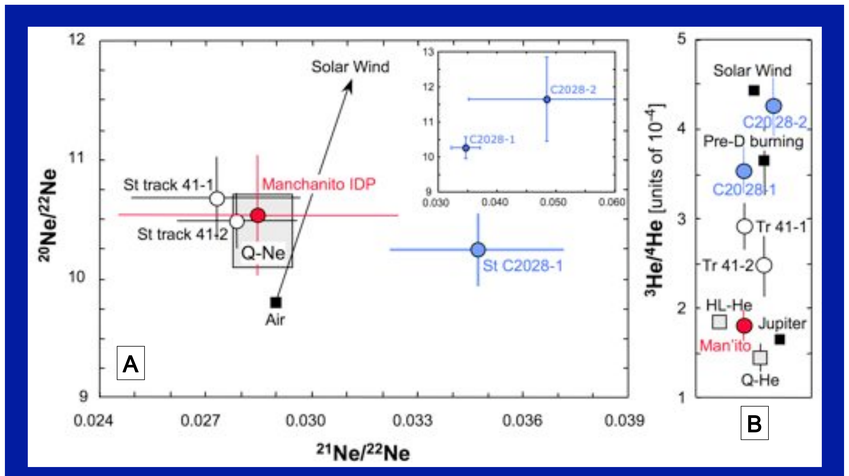

Fig. 3. (A) Neon composition in C2028-1 compared to those found in Stardust track 41 [2] and the "Manchanito" particle from the L2071F1 cluster IDP [8]. All three display $^{20}Ne/^{22}Ne$ ratios that fall within the Q-Ne data field [9]. However the $^{21}Ne/^{22}Ne$ ratio in C2028 is notably enhanced relative to Q-$^{21}Ne/^{22}Ne$, likely reflecting a spallogenic contribution. A second cell-surface sample, C2028-2 (Fig. 1), contained >10x less Ne than C2028-1, with a corresponding reduction in measurement precision as seen in the inset. The reason for its lower Ne content is unclear. Isotope ratios in the two samples are marginally compatible within errors.

(B) He ratios are elevated with respect to Q-$^{3}He/^{4}He$ in the Stardust track 41 and C2028 samples, suggesting addition of solar wind (SW) components. The possible presence of SW-He in the track 41 materials was considered by [2], and $^{3}He/^{4}He$ ratios resembling SW have been seen in surface samples adjacent to track 41 [4]. The higher $^{3}He/^{4}He$ in C2028 arguably reflects additions of both SW-He and spallation ^{3}He to an initially Q-like $^{3}He/^{4}He$ ratio.

Fig. 1. Noble gas measurements were carried out on samples ~100 μm thick and ~0.5 cm^2 in area keystoned from the cell C2028 surface, crushed and loaded in Pt foils, and degassed by step-heating to ~1400 °C. Details of the heating protocol used in the C2028 analyses are given in [5]. Sample sizes and their locations on the 2028 surface are shown in the figure.

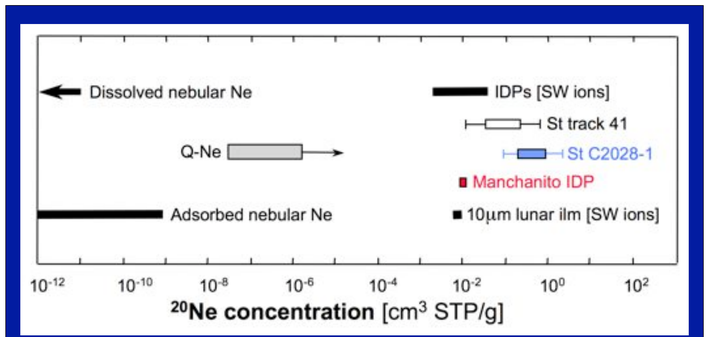

Fig. 4. A plot, updated from [2], of a group of high (≥ ~10^{-2} cc/g) ^{20}Ne concentrations measured in IDPs, Stardust track 41, and lunar regolith grains. The Q-Ne concentration, shown here as a lower limit, may actually be similarly high if its carrier comprises only a small fraction of the meteoritic carbonaceous matter in which it is found [9]. The Ne loading of Stardust C2028-1 (blue), obtained by dividing its measured abundance by the estimated grain mass present in the 0.5 cm^2 sample area, falls in this group. The assumed grain mass is that of 50 1 μm particles (1/mm^2); the blue box represents concentration variations for grain densities ranging from 1 to 4 g/cm^3. The principal uncertainty in the C2028-1 Ne loading is the estimated grain mass embedded in the sample. The right error bar reflects the possibility that the particles are coated with melted aerogel to the extent that their actual diameters are only half their average imaged size. The left limit is based on observations (see Fig. 5 and discussion) of crater populations in Al foil [10]. Other possibilities include a density of secondary particles well above ~1/mm^2 in the unscanned area from which the C2028-1 sample was taken. However a significantly higher track density, or the presence of larger particles which would severely increase the estimated mass, would have been observed during keystoning.

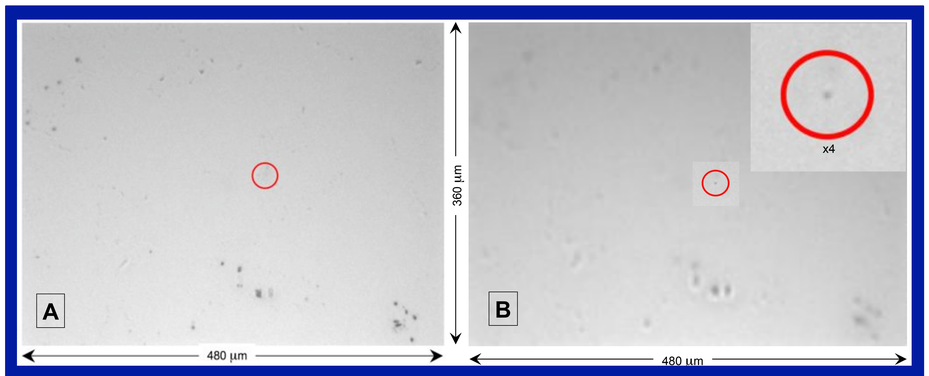

Fig. 2. Approximately 17% of the C2028 surface was scanned at JSC by ~770 high-resolution zoom-focus movies [6]. (A) A surface-focused frame from one movie. Surficial ~μm-size contaminant dust is apparent. Nothing is visible in the red circle, but with below-surface focus at ~50 μm depth (panel B) a probable track with an embedded ~1 μm particle appears (note defocused surface dust). The movie scans collectively revealed similar tracks and ~1 μm terminal particles at a density of ~1 per mm^2 of cell surface area. Track axes are off-normal to the cell surface and point toward the spacecraft's Whipple shield, indicating that the terminal particles are secondary fragments ejected during collision of a coma grain with the shield [7].

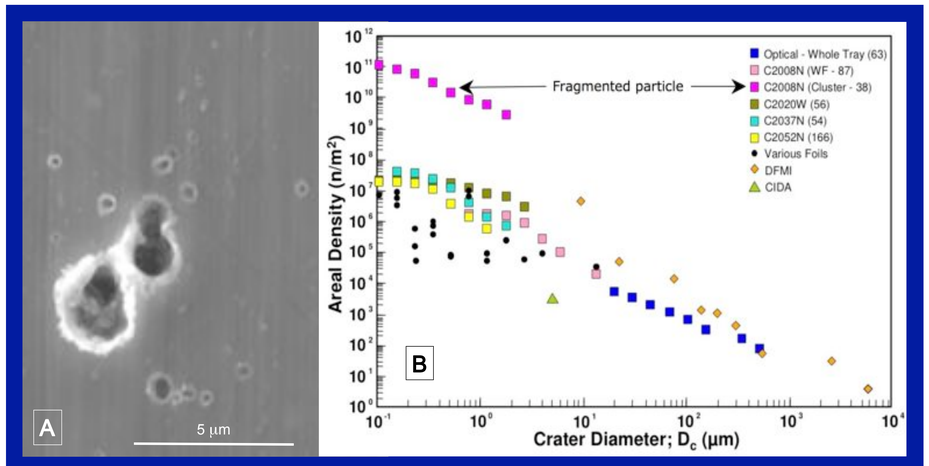

Fig. 5. Hörz et al. [10] reported comprehensive measurements of crater populations recorded on Al foil exposed to coma grain impacts on the comet dust collector array. A feature pictured in Fig. S5 in [10], observed on Al foil adjacent to aerogel cells C2008 and C2009, is reproduced in panel (A). Its crater distribution of descending sizes is interpreted by [10] as impacts of a recently disaggregated small parent particle. Interestingly, neighboring cell C2009 resembles C2028 in that it also carries a population of small off-normal tracks consistent with capture of a spray of secondary particles from a disaggregating collision of a coma grain with the Whipple shield [7]. Fig. S6 in [10], shown in panel (B), indicates that the density of small particles in (A) is orders of magnitude higher than that generated by direct primary particle impacts. From crater-projectile size scaling the largest impactor in (A) was a ~1 μm grain [10], comparable in size to the C2028 particles, but almost half the total mass of the debris field in (A) is carried by secondary fragments less than ~0.5 μm in size. These could have been implanted by impacts of similar secondary ejecta into the surface of cell C2028, but may have been generally too small for their tracks and terminal particles to be readily detectable at the movie scan resolution. An estimate of C2028-1 sample mass calculated from the data in (B) yields an approximately 2x lower ^{20}Ne concentration, marked by the end of the left error bar in Fig. 4.

Conclusions

The Q-Ne composition, hosted in a minor but gas-rich macromolecular organic phase ubiquitous in chondritic and achondritic meteorites [9], appears not to be confined to meteoritic "phase-Q". A Q-$^{20}Ne/^{22}Ne$ signature has now been seen in two Wild 2 comet coma samples, in the Manchanito IDP, and most recently in several grains from the U2-20GCA giant cluster IDP [11]. In none of these is there evidence, as yet, that the Q-Ne carriers are carbonaceous. A striking difference between the two comet samples is the elevated $^{21}Ne/^{22}Ne$ ratio in C2028 (Fig. 3A), pointing to a spallation component. As noted above, the high $^{3}He/^{4}He$ in C2028 (Fig. 3B) could also be due, in part, to spallogenic He. The calculated spallation ^{21}Ne concentration in C2028-1 is large, ~2 x 10^{-4} ccSTP/g. Division by a production rate appropriate to space irradiation of small grains [12] leads to an impossibly long exposure age unless particle exposure occurred near the young evolving sun in an environment of intense flare-generated radiation before their transport to comet-forming nebular regions, as discussed in [11]. Sample mass uncertainties, while large, are still too small to challenge the conclusion that the high Ne concentration in C2028-1, overlapping Stardust track 41 and falling in the same area of Fig. 4 as Manchanito, is due to Q-Ne ion implantation [2,8]. This mechanism produces the similarly large Ne loadings of SW-irradiated IDPs and lunar ilmenites shown in Fig. 4

References

[1] Palma R. L. et al. (2007) 38th LPSC, abstract #2032.
[2] Marty B. et al. (2008) *Science* **319**, 75.
[3] Palma R. L. et al. (2012) 43rd LPSC, abstract #1076.
[4] Palma R. L. et al. (2013) 44th LPSC, abstract #1084.
[5] Pepin R. O. et al. (2011) *ApJ* **742**, 2/86, 1.
[6] Westphal A. J. et al. (2014) *Meteoritics & Planet. Sci.* **49**, 1509.
[7] Westphal A. J. et al. (2008) *Meteoritics & Planet. Sci.* **43**, 415.
[8] Palma R. L. et al. (2013) 44th LPSC, abstract #1694.
[9] Busemann H. et al. (2000) *Meteoritics & Planet. Sci.* **35**, 949.
[10] Hörz F. et al. (2006) *Science* **314**, 1716.
[11] Pepin R. O. et al. (2015) This conference, abstract #1706.
[12] Reedy R. C. (1987) *Proc. 17th LPSC, Part 2*, E697.